

Micromachined Spatial Filters for Quantum Cascade Lasers

Abigail Hedden, Patrick Pütz, C. d'Aubigny, Dathon Golish, Christopher Groppi, Christopher Walker, Benjamin Williams, Qing Hu, and John Reno

Abstract—Quantum Cascade Lasers (QCL) are the most promising technology for producing compact, high power (> 1 mW), coherent signal sources above 2 THz. Due to their small size ($10 \mu\text{m} \times 25 \mu\text{m}$) and rectangular cross-section, the output beam from a QCL laser cavity is highly divergent and non-Gaussian. A single mode Gaussian beam is desirable for efficient coupling to optical systems. We have designed a waveguide spatial filter for this purpose. The 2.7 THz spatial filter consists of two diagonal feed horns connected by one wavelength of square waveguide ($92 \mu\text{m}$ on a side). The mode filtering efficiency and far field beam pattern of the structure have been modeled in CST Microwave Studio. We have fabricated the filter in tellurium copper using a Kern MMP micromilling machine. We present measurements of the QCL's throughput and emergent power pattern with and without the filter. Our preliminary findings suggest that spatial filtering significantly improves the QCL beam pattern, and further measurements are being made to more rigorously explore these results.

Index Terms—Quantum Cascade Lasers, waveguide spatial filters, terahertz, beam pattern.

I. INTRODUCTION

THERE is a growing need in the astronomical community for high frequency (>1 THz), high spatial and spectral resolution observations. Until recently, there has been a lack of high resolution astronomical data in the THz regime (1 THz – 10 THz) due to difficulties in constructing coherent receivers and the poor transmission of Earth's atmosphere at these frequencies. Space-based and airborne missions such as Herschel and SOFIA have spurred advances that have helped overcome some of these barriers, pushing the frontiers of heterodyne receiver technology to ~ 2 THz. Through diligent efforts of many researchers, astronomers are beginning to tap into the 1.3 and 1.5 THz atmospheric windows, obtaining spectroscopic observations of important tracers including high-J CO lines and the $205 \mu\text{m}$ [NII] line, e.g., [1]–[3]. Spectroscopy at THz frequencies is providing a wealth of information about the inner workings of our galaxy, encompassing

Manuscript received June 30, 2006. This work was partially supported by a NASA GSRP grant, no. NGT5-50463, to A. Hedden. P. Pütz is partially supported by DFG grano no. SFB494.

A. Hedden, P. Pütz, C. d'Aubigny, D. Golish, C. Groppi, & C. Walker are with Steward Observatory, University of Arizona, 933 N. Cherry Ave., Tucson, AZ 85721, USA (A. Hedden phone: 520-621-6535; fax: 520-621-1532; e-mail: ahedden@as.arizona.edu).

P. Pütz is also with KOSMA, I. Physikalisches Institut der Universität zu Köln, Zùlpicher Str. 77, 50937 Köln, Germany.

B. Williams & Q. Hu are with Department of Electrical Engineering and Computer Science & Research Laboratory of Electronics, Massachusetts Institute of Technology, Cambridge, MA 02139, USA.

J. Reno is with Sandia National Laboratories, Albuquerque, NM 87185, USA.

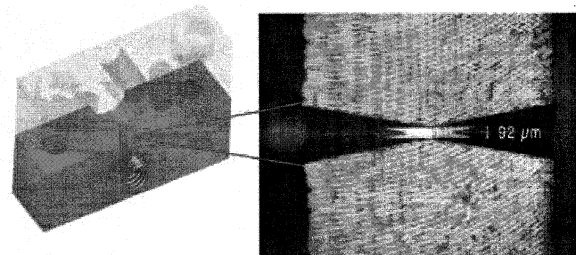


Fig. 1. Microscopic and CAD images of a split-block half of the 2.7 THz spatial filter structure. Two diagonal feed horns are connected by \sim one wavelength ($\lambda_g(\text{TE}_{10}) = 140 \mu\text{m}$) of $92 \mu\text{m}$ square waveguide.

protostellar cores, high-mass star formation, mechanisms of formation and destruction of molecular clouds, and life cycles of the galactic interstellar medium. These scientific goals continue to drive the developing technology toward higher frequencies and multi-pixel arrays.

Future missions will require spectroscopic capabilities at even higher frequencies (2 THz – 6 THz), e.g., [4]. The development of heterodyne instruments operating in this region depends upon the availability of coherent LO sources. At these frequencies, current solid state LO chains may not be capable of providing sufficient power much above 2 THz [5]. Although gas lasers operating in the far infrared and THz regime can supply sufficient mixer pumping power, their size, weight, and operation requirements limit their utility. QCL devices are the most promising technology for LO sources above 2 THz.

The small physical size ($10 \mu\text{m} \times 25 \mu\text{m}$) and rectangular cross-section of QCL devices lead to highly divergent, non-Gaussian emergent power patterns ([6], [7], and this work). Laboratory HEB-QCL receiver tests have been conducted at 2.8 THz [8] and 2.5 THz [9], but with relatively inefficient LO-receiver optical coupling. We have designed, fabricated, and tested a 2.7 THz waveguide spatial filter that transforms the output of a QCL into a well-behaved Gaussian beam, thereby permitting the implementation of efficient optical systems.

II. QCL WITH MICROMACHINED SPATIAL FILTER

A. Micromachined Spatial Filter

Hollow metallic waveguide devices have proven themselves as efficient spatial filters in the far infrared and THz regimes. Such a filter, machined at MIT Lincoln Laboratory, was assembled and measured at 2 THz in Steward Observatory

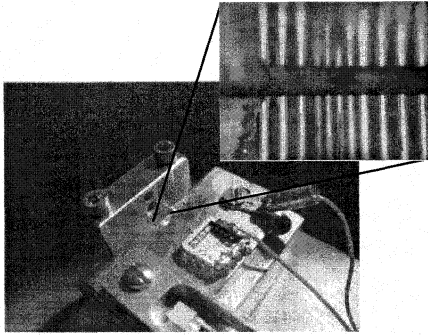


Fig. 2. Microscope image of QCL aligned with diagonal feed horn (illumination through feed horn). View of QCL chip and spatial filter mounted on cold finger of LN2 cryostat along with temp. sensor and device electrical connections.

[10]. These devices have been fabricated to frequencies as high as 5 THz using silicon laser micromachining techniques [11]. Recently, we have designed and metal machined a 2.7 THz spatial filter, consisting of two diagonal feed horns ($380 \mu\text{m}$ aperture) arranged back-to-back and connected with one wavelength ($\lambda_g(\text{TE}_{10}) = 140 \mu\text{m}$) of square waveguide ($92 \mu\text{m} \times 92 \mu\text{m}$, $170 \mu\text{m}$ long).

Feedhorns provide very efficient coupling ($\sim 98\%$) for incident Gaussian beam modes, while coupling very poorly to any non-Gaussian components. The short section of waveguide between the feed horns is designed to provide excellent modal filtering; suppressing non-fundamental Gaussian modes by 6 orders of magnitude or more [12]. Spatially filtered signals then exit the device via the other feedhorn. In this manner, the designed filter not only passes Gaussian components from the divergent and non-Gaussian QCL emergent beam, but also, it ensures that the spatial filter output is single-moded. The far-field beam pattern of the filter's output was modeled in CST MWS and the device was micromilled in tellurium copper using a Kern MMP machine at Steward Observatory. Figure 1 shows CAD and microscopic images of the milled spatial filter cross-section.

B. QCL Chip

The QCL device used in these measurements was designed at MIT's Research Laboratory of Electronics and fabricated at Sandia National Laboratory. It uses a lower radiative level depopulation technique achieved through resonant tunnelling and LO-phonon scattering [13]. Mode confinement is accomplished with a low-loss, double-sided metal-metal waveguide fabricated via copper-to-copper thermocompression bonding [14]. Combined, these features permit a high CW operating temperature (110 K for device used in this work) and long lasing wavelengths (2.66 THz or 2.75 THz depending on bias). Figure 2 shows a microscopic image of the QCL chip and device used in this work. The active volume of the device is $19 \mu\text{m} \times 800 \mu\text{m} \times 10 \mu\text{m}$ (width, length, and height, respectively) and $380 \mu\text{W}$ output power was detected at 5 K operation with a Pyro detector and Winston cone mounted in front of the $19 \mu\text{m}$ device facet.

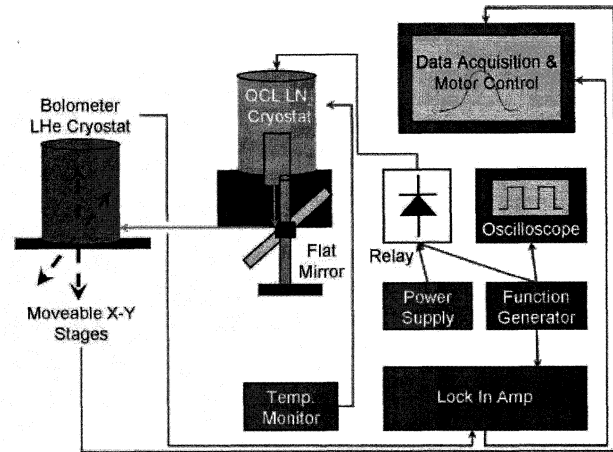


Fig. 3. Schematic of the measurement setup used to produce the presented beam patterns and cross-cuts. A 4.2 K Si bolometer mounted on moveable X-Y stages was used as a detector. The QCL device was electrically chopped with a 22 Hz square wave and was mounted on cold finger extension of a LN2 cryostat, operated under stable temperature conditions. Motions of the X-Y stages were controlled by a computer that also recorded the output of the lock-in amplifier used during measurements.

III. MEASUREMENT SETUP

Figure 2 shows the orientation of the QCL with respect to the spatial filter during beam pattern measurements. The QCL chip is indium soldered to a slotted copper mounting plate that was carefully aligned under a microscope so that the $19 \mu\text{m}$ device facet faces the spatial filter's input diagonal horn. This assembly was mounted to a copper cold finger of a LN2 dewar and the temperature of the cold finger mount was monitored (81 K) to ensure stability during operations. The QCL chip and spatial filter were enclosed in a metal cavity for beam pattern measurements in order to reduce the risk that QCL radiation not coupling into the filter could leak through the cryostat window, resulting in spurious measurements.

Figure 3 is a schematic of the measurement setup used to produce the beam patterns presented in this work. The QCL device was electrically chopped with a 22 Hz, 50% duty cycle square wave at 11.50 V and 27 mA. A 4.2 K Si bolometer with a Winston cone was used as a detector. The bolometer cryostat was mounted to moveable X-Y stages capable of traveling a total of 60 cm in each axis. The LN2 dewar was mounted on an optical table with a 45° flat mirror to direct QCL power toward the X-Y stages. The total optical path length with the detector at the peak intensity location was 62.5 cm (with 1.4 cm in vacuum). Mylar windows 0.5 mil thick and 0.5 inches in diameter were used for both cryostats. Eccosorb was placed around the window and housing of the bolometer dewar, the X-Y stages, optical table, and LN2 cryostat in order to curb reflections during measurements. A Stanford Research Systems SR830 DSP lock-in amplifier was used during measurements. All motions of the moveable stages were computer controlled. In order to allow for settling of the bolometer cryostat, a dwell time of 2 s was used before each measurement was made. The integration time per position was 2 s.

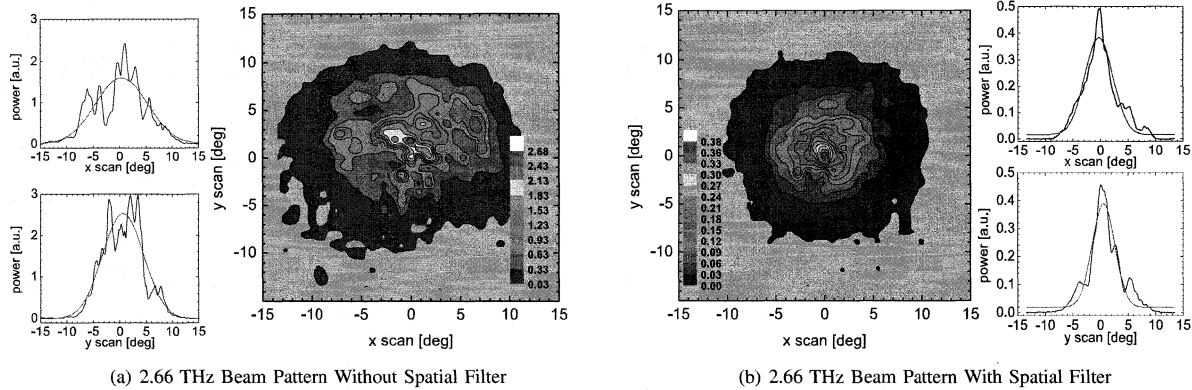


Fig. 4. Beam pattern measurements (2-D maps and high res. 1-D cross-cuts) at 2.66 THz of “bare” QCL (a) and QCL + spatial filter (b). Power is represented in arbitrary units. Resolution of 2-D maps is 0.9° and contours begin at 2σ and increase in 20σ steps to emission peak. Dynamic range achieved is 22 dB and 19 dB for measurements made with and without the spatial filter, respectively. High res. (0.2°) cross-cuts were made in two dimensions across the centers of each map. Gaussian fits to these cross-cuts yield 3 dB beam widths of 6.2° and 5.0° in “x” and “y” for measurements with the spatial filter and 11.6° and 9.2° for the “bare” QCL.

IV. RESULTS

With the described measurement setup, two dimensional (2-D) beam pattern measurements and high resolution 1-D cross-cuts were made with and without the spatial filter in front of the QCL device. The results are presented in Figure 4. Each of the 2-D beam pattern maps covers a total of 30 cm ($\sim 30^\circ$ with this experiment’s optical path) in each dimension and consists of raster-scanned measurements made at 1 cm spacing, resulting in 0.9° spatial resolution. The intensity scalings shown in the insets of Figure 4 represent power detected in arbitrary units, allowing for relative comparisons between data sets. The 2-D power patterns possess dynamic ranges of 22 dB and 19 dB for measurements made with and without the spatial filter, respectively. In addition, high resolution (0.2°) 1-D cross-cuts were made across the “x” and “y” centers of the maps.

Figure 4 indicates that spatial filtering improves the QCL beam pattern quality significantly. Measurements of the beam exiting the spatial filter show single-peaked, narrow features that are more Gaussian in shape than the unfiltered QCL output. For example, fitting Gaussian functions to the 1-D data yield 3 dB beam widths of 6.2° and 5.0° in “x” and “y” respectively for filtered measurements and 11.6° and 9.2° for the bare QCL. The throughput efficiency of the spatial filter is on the order of $\sim 10\%$; the ratio of peak power with and without the filter is 7% and the ratio of the integrated power within the 3 dB beam widths is 9%. This is a very encouraging preliminary result for telescope receiver and array applications, since $\sim 10\%$ of the QCL device’s output power is single-moded and Gaussian.

The strongest peak features appearing in the map and 1-D scans of the unfiltered data are repeatable and seem to be intrinsic to the QCL device’s output, supporting the interpretation that the observed output is divergent and non-Gaussian, potentially the result of internal interference [6]. Smaller peak features present in all data sets may partially arise from standing waves in the measurement setup. In

addition, there is a discrepancy in the 3 dB beam width of the spatial filter simulated in CST MWS (23.3°) and the measurements presented here (~ 5.0 – 6.2°). This mismatch is currently under investigation and has led us to redesign the QCL cold finger extension to permit a larger cryostat window and operation without the 45° flat mirror.

V. CONCLUSIONS AND OUTLOOK

We present a new method for improving the QCL beam pattern using waveguide spatial filters incorporating back-to-back feedhorns connected with square waveguide. We have designed, micromilled, and tested a 2.7 THz spatial filter with a resonant-phonon-assisted THz QCL device. We present 2-D maps and 1-D high resolution cross-cuts of power patterns with and without the spatial filter. Our results indicate that spatial filtering significantly improves the QCL beam pattern quality, with the emergent spatial filter signal being single peaked and more Gaussian. The measured throughput of the filter is $\sim 10\%$. Waveguide spatial filters provide a means of efficiently integrating QCLs into waveguide systems; e.g. power dividers, couplers, mixer blocks, etc. Silicon micromachining capabilities can extend the fabrication of waveguide spatial filters into the high THz range ([11]).

REFERENCES

- [1] M. C. Wiedner, G. Wieching, F. Biellau, K. Rettenbacher, N. H. Volgenau, M. Emprechtinger, U. U. Graf, C. E. Honingh, K. Jacobs, B. Vowinkel, K. M. Menten, L. Nyman, R. Güsten, S. Philipp, D. Rabanus, J. Stutzki, and F. Wyrowski, *Astronomy & Astrophysics manuscript no. 5341* (2006).
- [2] D. P. Marrone, R. Blundell, E. Tong, S. N. Paine, D. Loudkov, J. H. Kawamura, D. Lühr, and C. Barrientos, *16th Int’l Symp. on Space THz Tech.*, eds. J. Stake, H. Merkel, Göteborg, Sweden: Chalmers (2005).
- [3] D. P. Marrone, J. Battat, F. B. Besch, R. Blundell, M. Diaz, H. Gibson, T. Hunter, D. Meledin, S. Paine, D. C. Papa, S. Radford, M. Smith, and E. Tong, *Astrophysical Journal* **612**, 940 (2004).
- [4] Th. de Graauw, J. Cernicharo, W. Wild, A. Box, J-W. den Herder, A. Gunst, F. Helmich, B. Jackson, H-J. Langevelde, P. Maat, J. Martin-Pintado, J. Noordam, A. Quirrenbach, P. Roelfsema, L. Venema, P. Wesselius, and P. Yagoubov, *Proc. SPIE* **5487**, 1522 (2004).
- [5] I. Mehdi, E. Schlecht, G. Chattopadhyay, and P. H. Siegel, *Proc. SPIE* **4855**, 435 (2003).

- [6] A. J. L. Adam, I. Kašalynas, J. N. Hovenier, T. O. Klaassen, J. R. Gao, E. E. Orlova, B. S. Williams, S. Kumar, Q. Hu, J. L. Reno, *Appl. Phys. Lett.* **88**, 1 (2006).
- [7] S. Kohen, B. S. Williams, and Q. Hu, *J. Appl. Phys.* **97**, 053106 (2005).
- [8] J. R. Gao, J. N. Hovenier, Z. Q. Yang, J. J. A. Baselmans, A. Baryshev, M. Hajenius, T. M. Klapwijk, A. J. L. Adam, T. O. Klaassen, B. S. Williams, S. Kumar, Q. Hu, J. L. Reno, *Appl. Phys. Lett.* **86**, 244104 (2005).
- [9] H.-W. Hübers, S. G. Pavlov, A. D. Semenov, A. Tredicucci, R. Köhler, L. Mahler, E. E. Beere, E. H. Linfield, and D. A. Ritchie, *16th Int'l Symp. on Space THz Tech.*, eds. J. Stake, H. Merkel, Göteborg, Sweden: Chalmers (2005).
- [10] C. K. Walker, G. Narayanan, H. Knoepfle, J. Kapara, J. Glenn, A. Hungerford, T. M. Bloomstein, S. T. Palmacci, M. B. Stern, J. E. Curtin, *8th Int'l Symp. on Space THz Tech.*, eds. R. Blundell, E. Tong, Boston: Harvard University (1997).
- [11] C. Y. Drouët d'Aubigny, C. K. Walker, D. Golish, M. R. Swain, P. J. Dumont, P. R. Lawson, *Proc. SPIE* **4852**, Interferometry in Space, ed. M. Shao (2002).
- [12] C. Y. Drouët d'Aubigny, *Laser Chemical Etching of Waveguides and Quasi-optical Devices*, Ph.D. Dissertation, Univ. of Arizona (2003).
- [13] Q. Hu, B. S. Williams, H. Callebaut, S. Kohen, and J. L. Reno, *Semicond. Sci. Technol.* **20**, S228 (2005).
- [14] B. S. Williams, S. Kumar, Q. Hu, and J. L. Reno, *Electron. Lett.* **40**, 431 (2004).